ADVANCED MATERIALS

Supporting Information

for *Adv. Mater.,* DOI: 10.1002/adma.201501329

Simultaneous Nano- and Microscale Control of Nanofibrous Microspheres Self-Assembled from Star-Shaped Polymers

*Zhanpeng Zhang, Ryan L. Marson, Zhishen Ge, Sharon C. Glotzer, and Peter X. Ma**

Supporting Information

Simultaneous nano- and micro-scale control of nanofibrous microspheres self-assembled from star-shaped polymers with tunable architecture

Zhanpeng Zhang, Ryan L. Marson, Zhishen Ge, Sharon C. Glotzer and Peter X. Ma

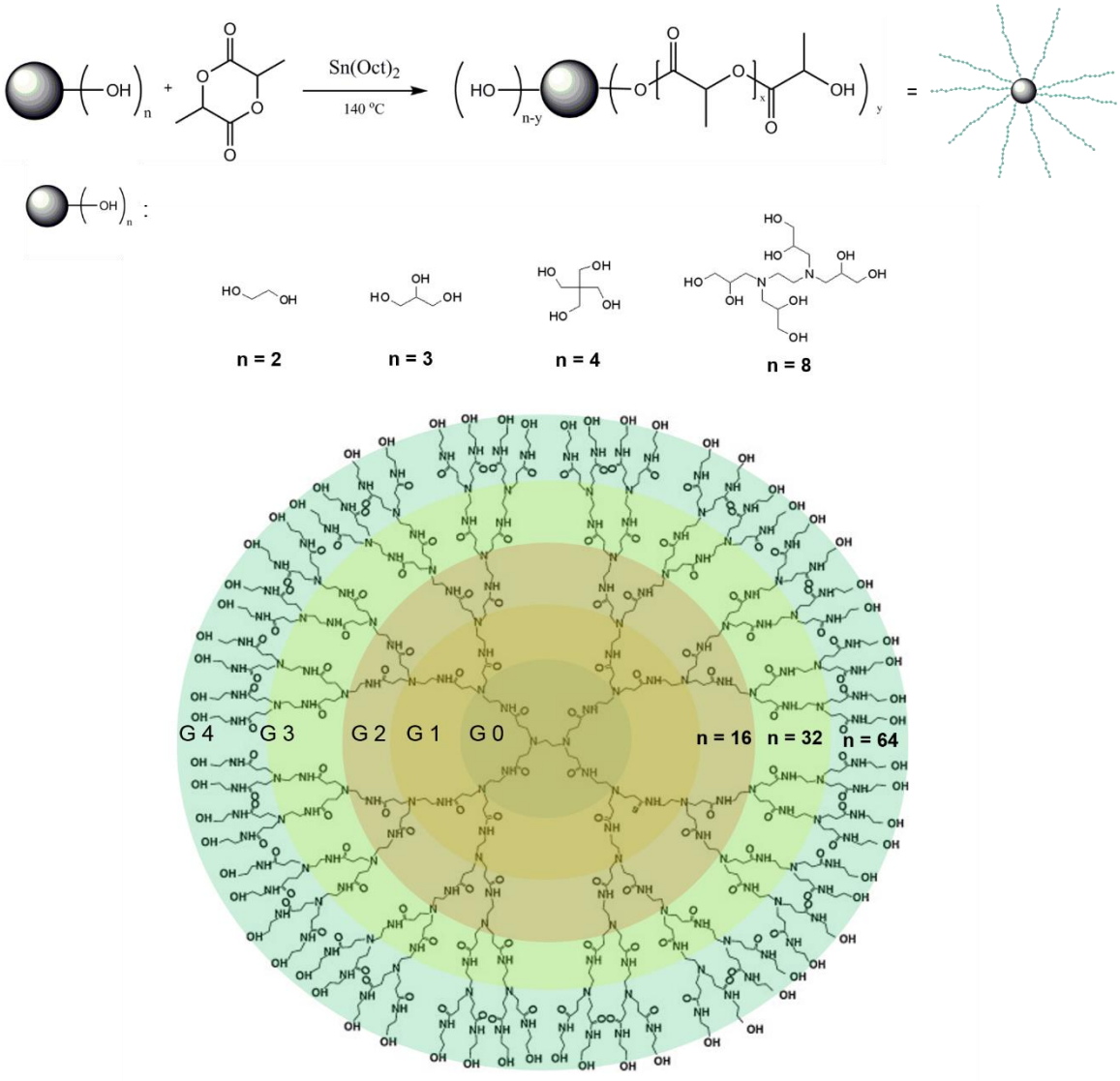

Figure S1. Synthesis route of SS-PLLAs from initiators with different number of initiating sites, including ethylene glycol (n=2), glycerol (n=3), pentaerythritol (n=4), N,N,N′,N′-tetra(2,3-dihydroxypropyl)ethane-1,2-diamine (n=8) and dendrimer PAMAM-OH (G2-OH (n=16), G3-OH

(n=32) and G4-OH (n=64)).

Table S1. Characterization of Star-shaped PLLA with Varying Arm Numbers[a]

Samples	Initiator[b]	X	Y	n[c]	DP[d]	Nano Structure	molecular weight		M_w/M_n[g]
							$M_{n,each}$[e]	$M_{n,total}$	
2-arm PLLA-150	ethylene glycol	2	150	2	220	--	15800	27700[f]	1.33
2-arm PLLA-200			200	2	250	NF	18000	31200[f]	1.40
2-arm PLLA-400			400	2	430	NF	31000	61700[f]	1.38
3-arm PLLA-150	Glycerol	3	150	3	200	--	14400	37200[f]	1.35
3-arm PLLA-200			200	3	230	NF	16600	47500[f]	1.34
3-arm PLLA-300			300	3	370	NF	26600	71400[f]	1.38
4-arm PLLA-50	Pentaerythritol	4	50	4	70	--	5000	15400[f]	1.48
4-arm PLLA-100			100	4	100	--	7200	21800[f]	1.44
4-arm PLLA-200			200	4	220	NF	15800	54800[f]	1.48
4-arm PLLA-400			400	4	400	NF	28800	108900[f]	1.49
8-arm PLLA-100	*N*,*N*,*N*′,*N*′-tetra(2,3-dihydroxypropyl)ethane-1,2-diamine	8	100	6	150	--	10800	65200[h]	--
8-arm PLLA-200			200	6	180	NF	13000	78400[h]	--
16-arm PLLA-100	PAMAM dendrimer (G_2-OH)	16	100	11	160	NF	11500	130000[h]	--
16-arm PLLA-400			400	12	450	NF	32400	392300[h]	--
32-arm PLLA-100	PAMAM dendrimer (G_3-OH)	32	100	20	140	NF	10100	216200[h]	--
64-arm PLLA-100	PAMAM dendrimer (G_4-OH)	64	100	36	200	NF	14400	532600[h]	--

[a]The polymerization conditions: $[Sn(Oct)_2]/[LA]=1/500$, at 135°C for 24 h. [b] Structures of the initiators are listed in Figure 1. [c] n is the NMR determined arm numbers, calculated from the average signal intensity ratios of reacted methylene protons of the initiator (4.27 ppm) to the unreacted methylene protons (3.59 ppm), combined with the number of surface hydroxyl groups (rounded to 1). [d] DP is the NMR determined average arm length, estimated by comparison of the integrals of methine protons (5.17 ppm) and the terminal methine (4.36 ppm) in SS-PLLA from ^{1}H NMR spectra (rounded to 10). [e] $M_{n,each}$ is the NMR determined average molecular weight of each arm, calculated by 72×DP (rounded to 100). [f,g] Obtained from GPC analysis using polystyrene as standard and THF as eluent. [h] The total MW of SS-PLLA with X≥8 is estimated from $Mn(NMR)= M_{n,each}\times n+MW_{initiator}$ (rounded to 100) instead of using GPC data, considering the inaccuracy of GPC in analyzing the total molecular weight of highly branched polymers.

Table S2. Characterization of the Microspheres Fabricated from Linear and Star-Shaped PLLA with Varying Arm Numbers[a]

microspheres	surface area (m^2/g)	porosity (%)	overall density (g/cm^3)	degree of crystallinity (%)
2-arm PLLA-150	1.3 ± 0.2	10.1	1.071	10.0
2-arm PLLA-400	110.4 ± 1.0	90.1	0.127	18.7
3-arm PLLA-150	1.9 ± 0.5	16.7	1.020	11.2
3-arm PLLA-300	109.7 ± 0.9	88.3	0.150	19.0
4-arm PLLA-50	4.3 ± 1.1	25.1	0.966	12.2
4-arm PLLA-100	120.4 ± 0.8	94.8	0.067	15.6
4-arm PLLA-300	112.3 ± 1.4	91.9	0.104	18.9
4-arm PLLA-400	121.1± 2.5	89.1	0.139	18.0
8-arm PLLA-300	118.4 ± 1.1	95.6	0.057	19.3
16-arm PLLA-50	89.5 ± 1.7	95.0	0.060	13.2
16-arm PLLA-100	120.8 ± 1.3	95.2	0.062	16.7
16-arm PLLA-200	121.7± 2.0	95.7	0.059	15.9
16-arm PLLA-500	118.8 ± 1.6	94.1	0.075	19.2
16-arm PLLA-700	124.0 ± 1.3	92.0	0.103	20.1
32-arm PLLA-100	119.2 ± 1.9	98.0	0.020	18.7
32-arm PLLA-600	120.8 ± 1.3	95.6	0.056	21.0
32-arm PLLA-700	124.2 ± 2.7	90.3	0.124	20.6
64-arm PLLA-100	111.8 ± 2.3	97.5	0.020	20.2
64-arm PLLA-200	117.2 ± 2.1	94.4	0.072	19.6
64-arm PLLA-400	120.7± 1.5	95.2	0.062	19.6
64-arm PLLA-600	118.1 ± 1.7	96	0.051	20.1
64-arm PLLA-700	115.6 ± 1.9	91.4	0.110	22.6

[a]All microspheres were fabricated according to the procedures described in the experimental section.

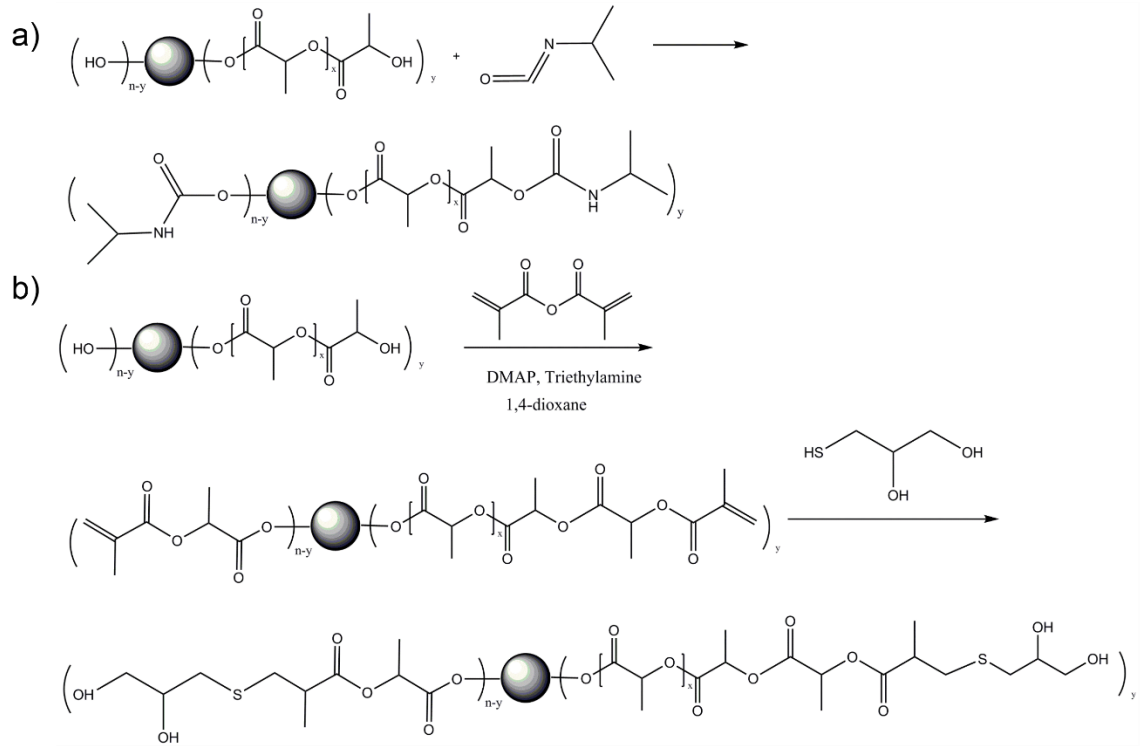

Figure S2. Hydroxyl capping (a) and doubling (b) reactions on SS-PLLAs.

Table S3. OH/LLA* values for Linear and Star-Shaped PLLAs with Varying Arm Numbers

Arm Number	**OH/LLA* for Non-Hollow to Hollow**	**OH/LLA* for Hollow to Spongy**
2	N/A	N/A
3	1/200	N/A
4	1/300	N/A
8	1/300	N/A
16	1/700	1/50
32	1/700	1/150
64	1/700	1/150

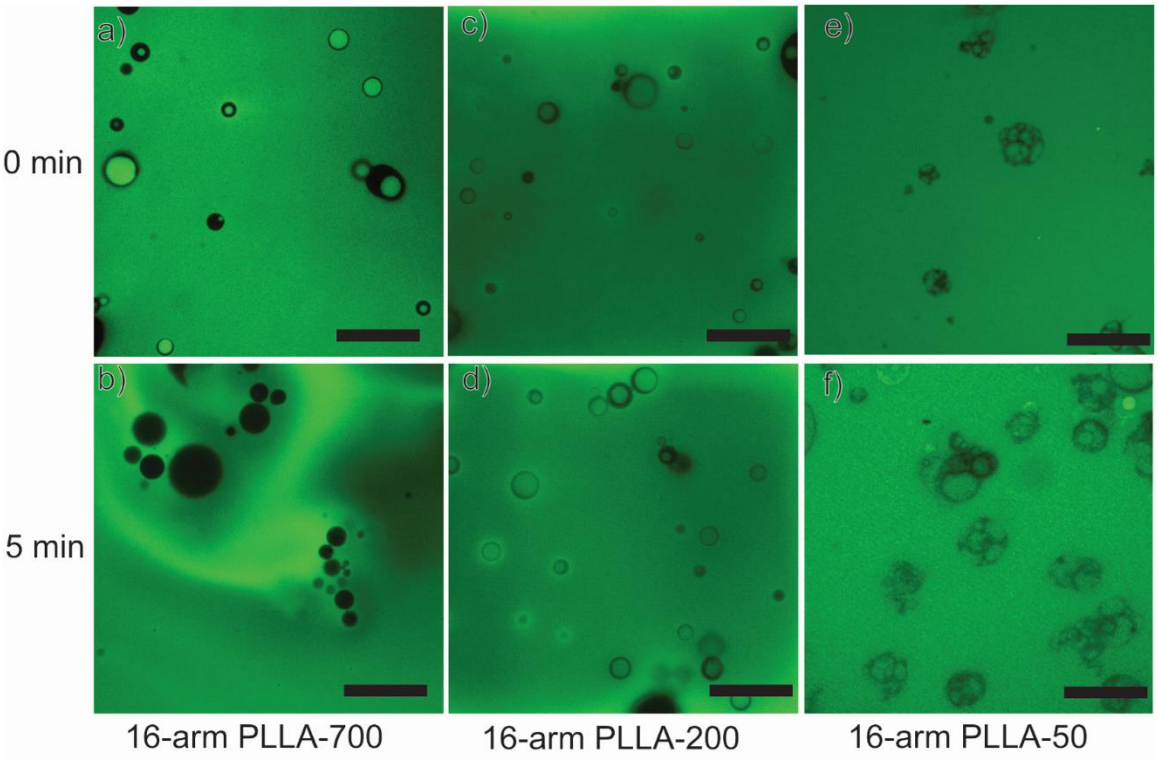

Figure S3. Fluorescence images of different emulsion systems at different time points. (**a, b**) For 16-arm PLLA-700, double emulsions (and some single emulsions) formed right after phase inversion (**a**), which transitioned into single emulsions at 5 min (**b**). (**c-d**) For 16-arm PLLA-200, double emulsions formed right after phase inversion (**c**), which were stabilized at 5 min (**d**). (**e, f**) For 16-arm PLLA-50, multiple emulsions formed right after phase inversion (**e**), which remained stable after 5 min (**f**). Scale bars: 100 μm.

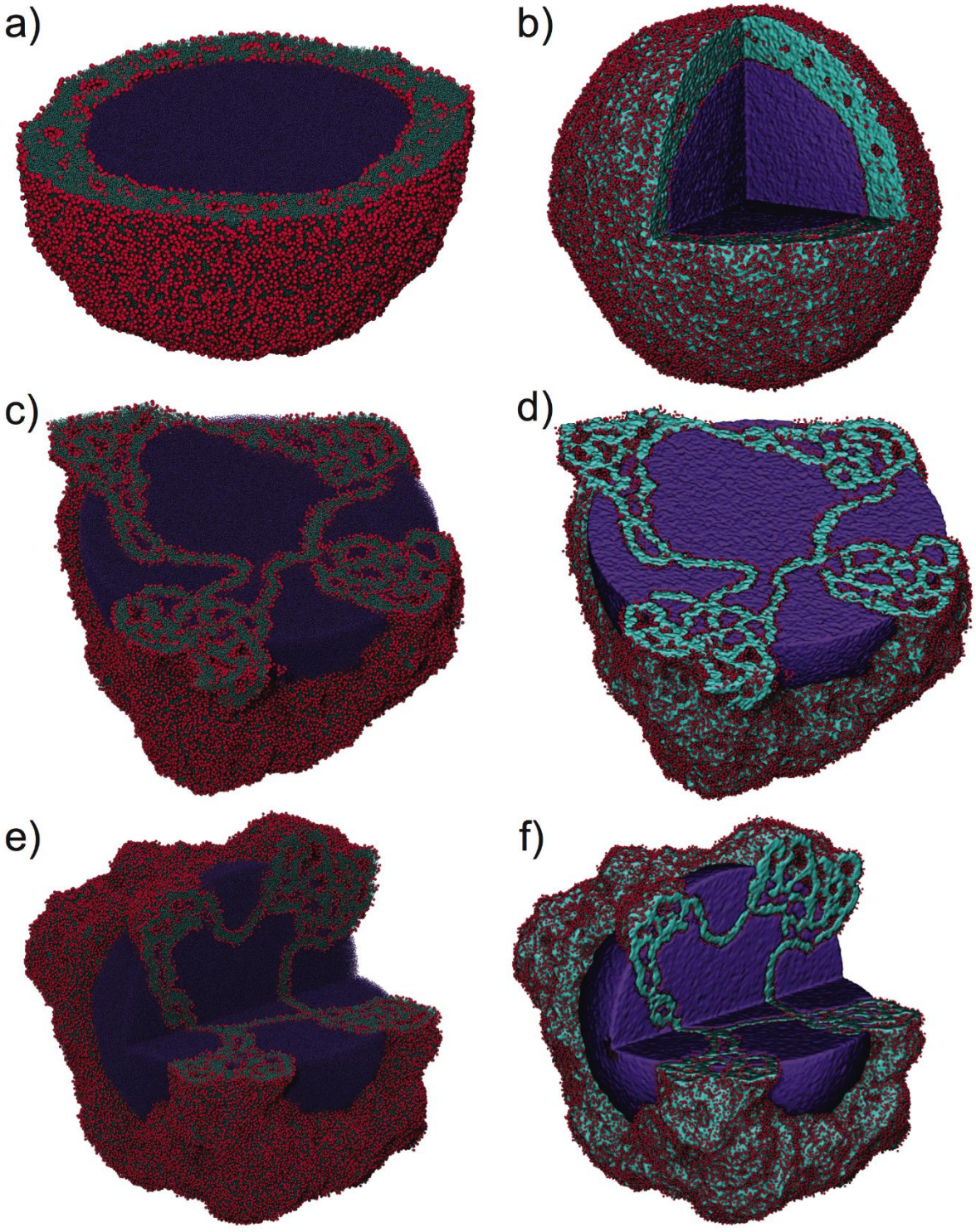

Figure S4. Large scale DPD simulations of 16-arm star-shaped polymers of varying arm length (containing ~11 million particles) and the formation of different emulsions: **a,b)** the formation of hollow structure at N_{bead}=40; **c-f)** the formation of spongy structure at N_{bead}=10. *Left* column shows individual bead representations, while the *right* shows the isosurface.

Supplemental Experimental Section

Materials.

Ethylene glycol (≥ 99%, Sigma-Aldrich) was dried over CaH_2 and distilled just prior to use. Glycerol (≥ 99%, Sigma-Aldrich) used as initiator was dried over 4 Å molecular sieves. Pentaerythritol and PAMAM-OH (G2-OH, G3-OH and G4-OH, Sigma-Aldrich) were dried over P_4O_{10} in a vacuum oven just prior to use. Tin(II) 2-ethylhexanoate ($Sn(Oct)_2$, 95%, Sigma-Aldrich), glycerol (≥ 99%, Sigma-Aldrich) as solvent in emulsification, isopropyl isocyanate, 1-thioglycerol, 4-dimethylaminopyridine, methacrylic anhydride, triethylamine, dimethyl sulfoxide (DMSO) and all other reagents were used as received. (3*S*)-*cis*-3,6-Dimethyl-1,4-dioxane-2,5-dione (L-lactide) (Sigma-Aldrich) was recrystallized from ethyl acetate twice and sublimated prior to use.

Sample Synthesis.

Synthesis of Initiator N,N,N′,N′-tetra(2,3-dihydroxypropyl)ethane-1,2-diamine. Glycidol (2.465 g, 33.28 mmol) was added dropwise into ethylenediamine (0.5 g, 8.32 mmol) over a period of 0.5 h at 0 °C. The reaction mixture was then stirred for 2 h at 0 °C. The product was collected and used without further purification. The product was characterized using ^{1}H NMR (δ, ppm, D_2O, Tetramethylsilane (TMS)): 4.11-3.81 (2H, C*H*OH), 3.73-3.45 (4H, CH_2OH), 2.96-2.50 (6H, CH_2N); and also characterized using Electrospray ionization mass spectrometry (**ESI-MS**): ($C_{14}H_{32}O_8N_2 + H^+$): calculated value = 356.4; experimental value = 357.3.

Synthesis of Star-Shaped PLLA with hydroxyl end groups (SS-PLLA-hydroxyl). Star-shaped PLLA was prepared via ring-opening polymerization (ROP) of L-lactide. Typical procedures employed for the preparation of 2-arm (linear) PLLAs were as follows. To a dried glass ampule equipped with a magnetic stirring bar, ethylene glycol (2.7 mg, 4.34×10^{-2} mmol), $Sn(Oct)_2$ (17.6 mg, 4.34×10^{-2} mmol), and L-lactide (5 g, 34.7 mmol) were added. After purging six times with dry nitrogen, the ampule was sealed under vacuum, and placed in an oil bath thermostated at 135 °C. After 24 h, the reaction mixture was dissolved in chloroform, precipitated into an excess of methanol. After filtration, the above dissolution-precipitation cycle was repeated three times. After drying in a vacuum oven overnight at room temperature, linear PLLA was obtained as a white solid (4.3 g, yield: 86.0%; $M_{n,GPC}$ = 61.7 kDa, M_w/M_n = 1.38). According to similar procedures, the star-shaped PLLA were prepared using glycerol, pentaerythritol, *N,N,N′,N′*-tetra(2,3-dihydroxpropyl)ethane-1,2-diamine, PAMAM dendrimers (G2-OH, G3-OH, or G4-OH) as the initiators, which were

denoted as 3-arm PLLA, 4-arm PLLA, 8-arm PLLA, 16-arm PLLA, 32-arm PLLA, and 64-arm PLLA, respectively. The characterization of the obtained polymers is summarized in **Table S1**.

Synthesis of SS-PLLA-isopropyl. SS-PLLA-hydroxyl (5 mmol hydroxyls) was dissolved in 1,4-dioxane under stirring. Isopropyl isocyanate (10 mmol, 0.850g) was then added into the solution and the reaction was carried out at room temperature for 2 hr. The mixture was then precipitated by ethyl ether. After filtration, the above dissolution-precipitation cycle was repeated three times. The polymer precipitate was then dried under vacuum for three days at room temperature, and characterized using Nuclear Magnetic Resonance Spectroscopy (^{1}H NMR) (δ, ppm, CD_3Cl, Tetramethylsilane (TMS)): 5.17 (-C(O)C*H*(CH_3)O-), 4.25 (terminal C(O)-C*H*(CH_3)-OH), 1.38 (-C(O)CH(C*H*$_3$)O-), 1.35 (terminal C(O-CH(C*H*$_3$)-OH), 4.36 (-CO-N(H)-C*H*(CH_3)$_2$), 1.28 (-CO-N(H)-CH(C*H*$_3$)$_2$).

Synthesis of SS-PLLA-vinyl. SS-PLLA-hydroxyl (5 mmol hydroxyls), methacrylic anhydride (10 mmol, 1.542 g), DMAP (10 mmol, 1.222 g) and TEA (10 mmol, 1.012 g) were dissolved in 1,4-dioxane (200ml) and stirred at room temperature overnight. The filtered solution was precipitated by adding ethyl ether. The dissolution-precipitation cycle was repeated three times. The polymer precipitate was then dried under vacuum for three days at room temperature, and characterized using ^{1}H NMR (δ, ppm, CD_3Cl, Tetramethylsilane (TMS)): 5.81-6.42 (C***H***$_2$=C(***H***)-), 5.17 (-C(O)C*H*(CH_3)O-), 4.25 (terminal C(O)-C*H*(CH_3)O-), 1.38 (-C(O)CH(C*H*$_3$)O-), 1.35 (terminal C(O)-CH(C*H*$_3$)O-).

Synthesis of SS-PLLA-diol. SS-PLLA-vinyl was dissolved in DMSO. Under stirring, 1-thioglycerol was added into the solution and the reaction was allowed to proceed for two hours. The mixture was then precipitated by methanol. After filtration, the above dissolution-precipitation cycle was repeated three times. The polymer precipitate was then dried under vacuum for three days at room temperature, and characterized using ^{1}H NMR (δ, ppm, CD_3Cl, Tetramethylsilane (TMS)): 5.17 (-C(O)C*H*(CH_3)O-), 4.23 (-S-CH-C*H*(OH)-CH_2(OH)), 4.30 (terminal C(O)-C*H*(CH_3)O-), 2.34-3.76 (-CO-C*H*$_2$-C*H*$_2$-S-CH-CH(OH)-C*H*$_2$(OH)), 1.38 (-C(O)CH(C*H*$_3$)O-), 1.35 (terminal C(O)-CH(C*H*$_3$)O-).

Characterization.

Nuclear Magnetic Resonance (NMR) Spectroscopy. ^{1}H NMR spectra were recorded on an Inova 400 NMR spectrometer operated in the Fourier transform mode. $CDCl_3$ and D_2O were used as

solvents. TMS was used as an internal reference.

*Electrospray Ionization Mass Spectrometry (**ESI-MS**)*. ESI-TOF mass spectra were acquired on a LCT mass spectrometer from Micromass (Manchester, U.K.). This instrument combines an electrospray ionization source with a TOF (time-of-flight) mass analyzer. The LCT mass spectrometer was used in the positive ionization mode for the experiments.

Gel Permeation Chromatography (GPC). The molecular weights (MWs) and MW distributions of the polymers were determined by GPC, which uses a series of three linear Styragel columns (HT2, HT4, and HT5). The eluent was THF at a flow rate of 1.0 mL/min. A series of low polydispersity polystyrene standards was employed for GPC calibration.

Scanning Electron Microscopy (SEM). The surface morphology of the microspheres was observed using SEM (Philips XL30 FEG). The samples were coated with gold using a sputter coater (DeakII, Denton vacuum Inc) for 120 seconds. During the process of gold coating, the gas pressure was kept at 50 mtorr, and the current was 40 mA. Samples were analyzed at 10 kV.

Surface Areas. The surface areas of various microspheres were measured via N_2 adsorption experiments at liquid nitrogen temperature on a Belsorp-Mini adsorption apparatus (Bel Japan Inc., Japan) after evacuating the samples at 25 ºC for 10 hours ($< 7 \times 10^{-3}$ Torr). The surface areas were calculated from a Brunauer-Emmett-Teller (BET) plot of adsorption/desorption isotherm using adsorption points in the P/P_0 range of 0.1-0.3 (BELSORP-mini analysis software).

Porosity ε. The porosity of the microspheres was calculated from $\varepsilon = 1-D_p/D_0$, where D_p is the overall density of the polymer microsphere aggregation and D_0 is the density of the solid polymer. D_p was determined from $D_p = 4m/(\pi d^2 h)$, where m, d, and h are mass, diameter, and thickness, respectively, of the microsphere aggregation in a disc-shaped container.

Confocal Imaging. The internal structure of hollow and spongy nanofibrous microspheres was observed using confocal laser scanning microscopy (CLSM) (Nikon Eclipse C1). The FITC-conjugated BSA was deposited throughout the microspheres and observed under confocal microscopy.

The emulsion structure was also observed through CLSM. Glycerol was stained with FITC and the polymer solution was not labeled. After phase inversion, the emulsions were stirred for i) 0 minutes and ii) five minutes before added into liquid nitrogen for phase separation at -76 ºC for

four hours. The specimen was cut into slices with a thickness of 100 μm at -20 ºC using a Cryostat and was quickly observed.

Degree of crystallinity X_c

The melting behavior of the microspheres was characterized with a differential scanning calorimeter (DSC-7; Perkin-Elmer, Norwalk, CT). The calibration was performed using indium standards. The microspheres after freeze-drying (2-10 mg) were used without further thermal treatment. A heating rate of 20°C/min and a temperature range of 30°-200°C were used. The degree of crystallinity was calculated as $X_c = \Delta H_m / \Delta H_m^o$, where ΔH_m was the measured enthalpy of melting and ΔH_m^o was the enthalpy of melting of 100% crystalline polymer. For PLLA, $\Delta H_m^o = 203.4 J/g$.

Detailed simulation section

$$
\begin{aligned}
F &= F_{\mathrm{C}}(r) + F_{\mathrm{R,ij}}(r_{ij}) + F_{\mathrm{D,ij}}(v_{ij}) \\
F_{\mathrm{C}}(r) &= A \cdot w(r_{ij}) \\
F_{\mathrm{R,ij}}(r_{ij}) &= -\theta_{ij}\sqrt{3}\sqrt{\tfrac{2k_b\gamma T}{\Delta t}} \cdot w(r_{ij}) \\
F_{\mathrm{D,ij}}(r_{ij}) &= -\gamma w^2(r_{ij})\,(\hat{r}_{ij} \cdot v_{ij}) \\
w(r_{ij}) &= (1 - r/r_{\mathrm{cut}}) \qquad r < r_{\mathrm{cut}} \\
&= 0 \qquad r \geq r_{\mathrm{cut}}
\end{aligned}
$$

Figure S5. Constitutive equations for the dissipative particle dynamics model. Conservative, random, and dissipative forces are applied pairwise at each timestep.

DPD Model details – Our DPD model is adapted from past studies of a similar nature [1, 2]. In this model, three forces are applied to each particle at each time step – a conservative, a random, and a dissipative force. The form of all three of these forces is shown **Figure S5**. The **conservative** force, $\boldsymbol{F_c}$, is a purely repulsive force meant to inhibit overlap between particles; the strength of this force is tuned through the coefficient *A*, allowing particles to be less or more repulsive. A pairwise **random** force, $\boldsymbol{F_R}$, mimics the effect of the solvent on the non-solvent beads. The **dissipative** force, $\boldsymbol{F_D}$, tunes the effective viscosity of the system by opposing the motion of the particle. Because the forces are applied pairwise, the DPD system is momentum conserving (S1).

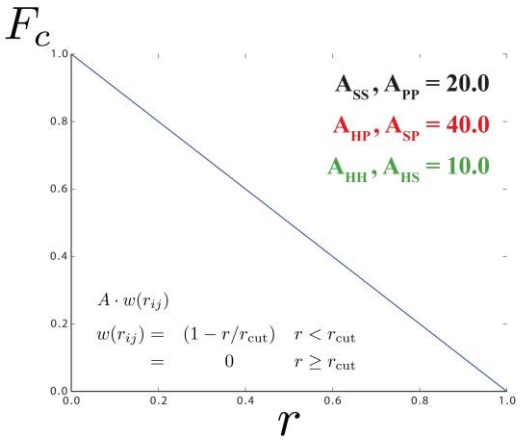

Figure S6. Pair coefficients for the conservative pair force A varies w/ type.

The coefficients for $\boldsymbol{F_c}$ between polymer beads (A_{PP}) and between glycerol (solvent) beads (A_{SS}) were set at $A_{PP} = A_{SS} = 20.0$ as a baseline, as has been done in prior works [2, 3]. To increase

affinity for the hydroxyl and solvent (glycerol), this repulsion was reduced to A_{HS} = 10.0, thereby making the hydroxyls attractive to the solvent. The repulsion between hydroxyls was also reduced to A_{HH} = 10.0, so that the hydroxyls have the same tendency to aggregate with other hydroxyls or at the glycerol-polymer solution interface. Because the hydroxyl-polymer and polymer-solvent interaction is repulsive, we increased the repulsion to $A_{HP} = A_{PS}$ = 40.0 (**Figure S6**).

Star polymers are created by linking beads together with harmonic springs $V(r) = \frac{1}{2}k(r - r_0)^2$, with k = 4 and r_0 = 0. Arms are attached to a single polymer core bead.

The temperature in the simulations was set at a standard value of T = 1.0. The timestep was chosen to be dt = 0.01 as a compromise between integration stability and expediency of the simulation. All simulations were run for 5 million DPD timesteps. Systems were initialized by randomly placing one million solvent beads in a box at a volume fraction of 80%. Star polymers were generated randomly beforehand, and then placed individually in a spherical shell, allowing for overlaps between polymer and solvent beads. The box size remained fixed across all simulations. Systems were thermalized for 30 thousand timesteps, and then run for 5 million steps to equilibrate.

The amount of solvent was kept fixed at 1 million particles, while the concentration of polymer was varied. Simulations were performed for eight different polymer concentrations $\frac{N_{poly}}{N_{total}} = 30\%, 28\%, 25\%, 22\%, 19\%, 16\%, 13\%, \text{or } 10\%$. System sizes varied between 1.1 and 1.5 million particles, depending upon concentration. At each concentration, four different arm lengths were run: N_{bead} = 10, 40, 80, or 120 beads per arm. Finally, all simulations were performed for 4, 8, and 16 arms. In total, over 100 individual simulations were performed. A total of 20,000 GPU/CPU hours was employed for this study.

To verify the effect of the hydroxyl stabilizer, two non-hollow cases were tested separately: 8 arm, N_{bead} = 120 at polymer concentrations of both 10% and 13%. The strength of the hydroxyl-solvent and hydroxyl-hydroxyl repulsion was decreased, thereby increasing the preference for the hydroxyls to aggregate at the polymer/solvent interface. In all cases, A_{HS}, A_{HP} = 8.0, 5.0, 2.0, or 1.0. Reducing A triggered a hollow to non-hollow transition.

Additionally, the hollow and spongy morphologies were tested for scaling in larger systems. Both morphologies were run at a single randomly chosen state point in systems of over 11 million

particles for 5 million time steps, and showed identical morphologies to smaller scale systems.

Finally, to ensure reproducibility of the structures, three independent runs were conducted for 50 million time steps each using Blue Waters. These runs were also used to create the movies contained in the SI.

All simulations were performed using the DPD implementation in HOOMD-Blue, a free and open-source code developed and maintained at the University of Michigan (http:codeblue.umich.edu/hoomd-blue). Images of the droplets and movies were created using VMD, a free visualization package available online.

Movies (in separate files):

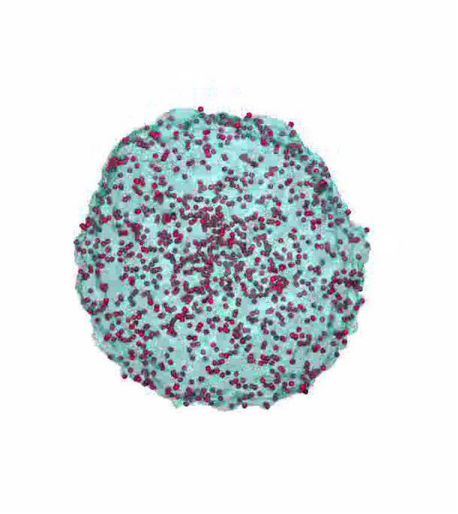

M1: A movie showing a single solution droplet of the star-shaped polymer with X=16, N_{bead}=120.

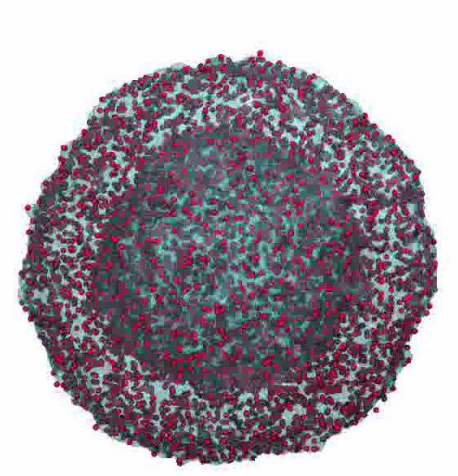

M2: A movie showing a single solution droplet of the star-shaped polymer with X=16, N_{bead}=40

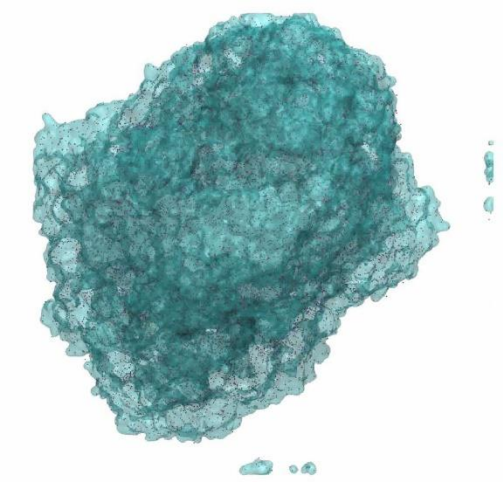

M3: A movie showing a single solution droplet of the star-shaped polymer with X=16, N_{bead}=10

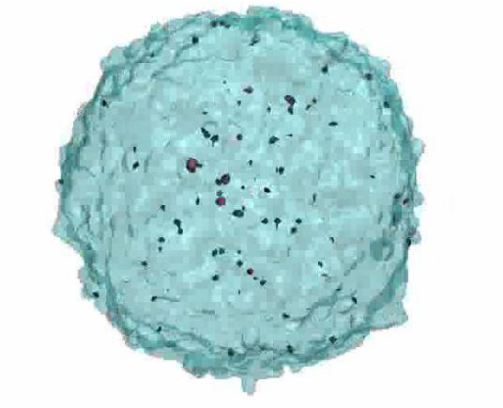

M4: A movie showing a single solution droplet of the star-shaped polymer with X=4, N_{bead}=40

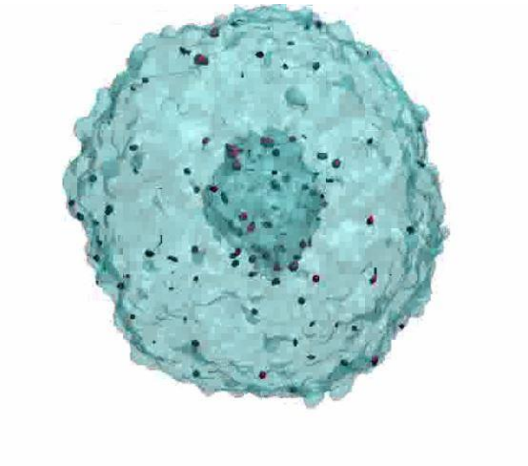

M5: A movie showing a single solution droplet of the star-shaped polymer with X=4, N_{bead}=40, and parameter A_{HS}=4 (mimicking the hydroxyl-doubling reaction).

References

[1] R. D. Groot, P. B. Warren, Journal of Chemical Physics 1997, 107, 4423.

[2] C. L. Phillips, J. A. Anderson, S. C. Glotzer, Journal of Computational Physics 2011, 230, 7191.

[3] J. Glaser, T. D. Nguyen, J. a. Anderson, P. Lui, F. Spiga, J. a. Millan, D. C. Morse, Glotzer, S. C. Computer Physics Communications, 2015; R. L. Marson, C. L. Phillips, J. A. Anderson, S. C. Glotzer, Nano Letters 2014, 14, 2071.